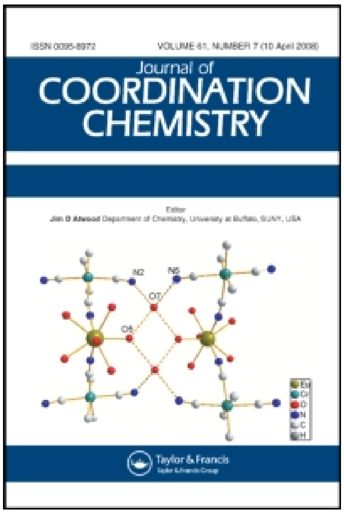

Journal of Coordination Chemistry
Publication details, including instructions for authors and subscription information:
http://www.informaworld.com/smpp/title~content=t713455674

Synthesis, crystal structure and properties of tungstoantimonates with Cu^{II} or Ni^{II} sandwiched by two [<i>α</i>-SbW_9O_{33}]$^{9-}$ or [<i>β</i>-SbW_9O_{33}]$^{9-}$ subunits

Ying-Hong Liu[a]; Peng-Tao Ma[a]; Jing-Ping Wang[a]
[a] Institute of Molecule and Crystal Engineering, School of Chemistry and Chemical Engineering, Henan University, Kaifeng 475001, P. R. China

To cite this Article Liu, Ying-Hong , Ma, Peng-Tao and Wang, Jing-Ping(2008) 'Synthesis, crystal structure and properties of tungstoantimonates with Cu^{II} or Ni^{II} sandwiched by two [<i>α</i>-SbW_9O_{33}]$^{9-}$ or [<i>β</i>-SbW_9O_{33}]$^{9-}$ subunits', Journal of Coordination Chemistry, 61: 6, 936 — 944, First published on: 22 September 2010 (iFirst)

To link to this Article: DOI: 10.1080/00958970701411403

URL: http://dx.doi.org/10.1080/00958970701411403

Journal of Coordination Chemistry
Vol. 61, No. 6, 20 March 2008, 936–944

Taylor & Francis
Taylor & Francis Group

Synthesis, crystal structure and properties of tungstoantimonates with Cu^{II} or Ni^{II} sandwiched by two [α-SbW$_9$O$_{33}$]$^{9-}$ or [β-SbW$_9$O$_{33}$]$^{9-}$ subunits

YING-HONG LIU, PENG-TAO MA and JING-PING WANG*

Institute of Molecule and Crystal Engineering, School of Chemistry and Chemical Engineering, Henan University, Kaifeng 475001, P. R. China

(*Received 9 February 2007; in final form 16 May 2007*)

Two sandwich-type tungstoantimonates $K_4Na_2H_3[Na_2K(H_2O)_2\{Cu(H_2O)\}_3(\alpha\text{-}SbW_9O_{33})_2]\cdot 15H_2O$ (**1**) and $Na_4H_4[\{Ni(H_2O)_3\}_2\{W(OH)_2\}_2\{\beta\text{-}SbW_9O_{33}\}_2]\cdot 23H_2O$ (**2**) were prepared from aqueous solution by different strategies. They were characterized by X-ray structure analysis, electrochemical analysis, EPR and IR spectroscopy. Both compounds are sandwich-like tungstoantimonates built from two *B*-[SbW$_9$O$_{33}$]$^{9-}$ building blocks. The polyoxoanion of **1** consists of two trivacant *B*-α-[SbW$_9$O$_{33}$]$^{9-}$ moieties linked by three Cu^{2+} ions leading to a Hervé-type sandwich framework. The polyoxoanion in **2** is composed of two isomeric *B*-β-[SbW$_9$O$_{33}$]$^{9-}$ subunits joined together by two Ni^{2+} and two W^{6+} ions resulting in a Krebs-type sandwich structure.

Keywords: Crystal Structure; Sandwich-type; Tungstoantimonate; Polyoxometalates

1. Introduction

Polyoxometalates (POMs), as a well-known class of metal-oxygen clusters, have attracted interest in different fields of chemistry including catalysis, material science, magnetism and medicine [1–3]. Numerous transition metal substituted POMs with topological beauty and a variety of properties were constructed, mostly from trivacant POMs building blocks [4]. To date, POMs built from *B*-α-[SbW$_9$O$_{33}$]$^{9-}$ or *B*-β-[SbW$_9$O$_{33}$]$^{9-}$ fragments are rare, and most are sandwich-type compounds. The mechanism of POM formation is still elusive and commonly described as self-assembly, because even large and complex structures (e.g. $[As_{12}Ce_{16}(H_2O)_{36}W_{148}O_{524}]^{76-}$) [5] can be synthesized in one-step reactions by interaction of the components rather than from a preformed polyoxoanion precursor. In addition, the obtained polyoxoanions usually exhibit novel structures and unexpected properties.

In transition metal substituted POM chemistry, the sandwich-type species are the largest subfamily [6]. To date Hervé- [7], Weakly- [8], Krebs- [9], and Knoth-type [10] sandwich polyoxoanions can be distinguished. Such compounds are usually obtained by reaction of transition metal ions (*e.g.* Cu^{2+}, Co^{2+}, Ni^{2+}) with the appropriate trivacant

---

*Corresponding author. Tel.: +86-378-2192443. Fax: +86-378-2850691. Email: jpwang@henu.edu.cn

Journal of Coordination Chemistry
ISSN 0095-8972 print/ISSN 1029-0389 online © 2008 Taylor & Francis
DOI: 10.1080/00958970701411403

POM precursor (e.g. $[PW_9O_{34}]^{9-}$, $[SiW_9O_{34}]^{10-}$, $[SbW_9O_{33}]^{9-}$ and $[P_2W_{15}O_{56}]^{12-}$). Recently, several new inorganic complexes containing two *B*-type $[SbW_9O_{33}]^{9-}$ anions linked by two or more transitions metal ions have been described [11, 12], which are of particular interest since the polyoxoanion building block $[SbW_9O_{33}]^{9-}$ contains a hetero group with a lone pair of electrons. Different from the tetrahedrally coordinated heteroatoms (e.g. P, Si, and Ge), the heteroatom Sb^{III} is surrounded pyramidally by three oxygen atoms. Though many polyoxometalates of this type have been reported, most of them were obtained from the trivacant precursor α-$[SbW_9O_{33}]^{9-}$. In this context, we obtained a K^+/Na^+ mixed salt $K_4Na_2H_3[Na_2K(H_2O)_2\{Cu(H_2O)\}_3(\alpha\text{-}SbW_9O_{33})_2]\cdot 15H_2O$ (**1**) using a different precursor, $[NaSb_9W_{21}O_{86}]^{18-}$, and a salt$Na_4H_4[\{Ni(H_2O)_3\}_2\{W(OH)_2\}_2\{\beta\text{-}SbW_9O_{33}\}_2]\cdot 23H_2O$ (**2**) without such a special precursor. In this work we focus on the EPR spectral and electrochemical results.

2. Experimental

$(NH_4)_{18}[NaSb_9W_{21}O_{86}]\cdot 24H_2O$ was prepared according to the literature method and identified by its IR spectrum [13]. All other chemicals were reagent grade and used without further purification.

2.1. *Preparation of* $K_4Na_2H_3[Na_2K(H_2O)_2\{Cu(H_2O)\}_3(\alpha\text{-}SbW_9O_{33})_2]\cdot 15H_2O$ *(1)*

10.70 g (0.15 mmol) $(NH_4)_{18}[NaSb_9W_{21}O_{86}]\cdot 24H_2O$ and 0.15 g (2 mmol) KCl were suspended in 20 mL of distilled water, to which 5 mL of a solution containing 1 mmol $CuCl_2\cdot 2H_2O$ was added dropwise under stirring. The resulting mixture was heated at 80°C under continuous stirring for 1.5 h and then allowed to cool to room temperature. After filtration, the filtrate was left to naturally evaporate at ambient temperature. Several days later, green cube crystals were obtained with high purity and yield. $H_{43}Cu_3K_5Na_4O_{86}Sb_2W_{18}$ (5450.22): Calcd K 3.59, Na 1.69, Cu 3.50, Sb 4.47, W 60.72; found: K 3.63, Na 1.71, Cu 3.44, Sb 4.51, W 60.54. IR (KBr pellets): $\nu = 943$ (s), 837 (vs), 769 (s), 710 (m), 669 (s), 493 (w), 469 (w) cm^{-1}.

2.2. *Preparation of* $Na_4H_4[\{Ni(H_2O)_3\}_2\{W(OH)_2\}_2\{\beta\text{-}SbW_9O_{33}\}_2]\cdot 23H_2O$ *(2)*

The raw materials $NiSO_4\cdot H_2O$ (0.33 g, 1.96 mmol), Sb_2O_3 (0.13 g, 0.444 mmol) and $Na_2WO_4\cdot 2H_2O$ (2.64 g, 8.0 mmol) were dissolved in 40 mL of 0.5 L^{-1} sodium acetate buffer (pH = 4.8) with stirring. The mixture was heated to 80°C for 1.5 h. Then the solution was cooled to room temperature and filtered. On slow evaporation of the clear solution in air, light green single crystals suitable for X-ray crystallography were obtained. $H_{66}Na_4Ni_2O_{99}Sb_2W_{20}$ (5780.41): Calcd Na 1.59, Ni 2.03, Sb 4.21, W 63.61; found: Na 1.61, Ni 2.04, Sb 4.15, W 63.34. IR (KBr pellets): $\nu = 949$ (s), 839 (vs), 774 (s), 669 (s), 469 (w) 453 (w) cm^{-1}.

2.3. *Physical measurements*

Inductively coupled plasma (ICP) analysis was performed on a Jarrel-Ash J-A1100 spectrometer. IR spectra were recorded in KBr pellets with a Nicolet 170 FT-IR

Table 1. Crystallographic data and structure refinement for **1** and **2**.

	1	**2**
Formula	$H_{43}Cu_3K_5Na_4O_{86}Sb_2W_{18}$	$H_{66}Na_4Ni_2O_{99}Sb_2W_{20}$
M_r	5450.22	5780.41
Crystal size (mm^3)	$0.14 \times 0.10 \times 0.08$	$0.14 \times 0.12 \times 0.11$
Crystal system	Orthorhombic	Monoclinic
Space group	$Pnma$	$P2_1/n$
a (Å)	30.2536(13)	12.890(5)
b (Å)	15.0639(7)	25.046(9)
c (Å)	19.1203(8)	15.978(6)
β (°)	90	94.491(5)
V (Å^3)	8713.8(7)	5142(3)
D (g cm^3)	4.154	3.733
Z	4	2
μ (Mo-Kα) (cm^{-1})	25.344	23.262
F(000)	9564	5080
θ range (°)	1.72 to 25.00	2.5 to 25.00
hkl range	$-35 \le h \le 35$, $-14 \le k \le 17$, $-22 \le l \le 22$	$-8 \le h \le 15$, $-28 \le k \le 29$, $-18 \le l \le 18$
Reflections measured	41533	22747
Reflections unique	7533	8593
R_{int}	0.1817	0.1816
GOF	1.041	0.997
Final R indices [$I \ge 2\sigma(I)$]	$R_1 = 0.0755$, $wR_2 = 0.1953$	$R_1 = 0.0709$, $wR_2 = 0.1955$

spectrometer in the 4000–400 cm^{-1}. EPR experiments were performed on a BrukerER-2000-DSRC10 spectrometer range (X-band) at 300 and 110 K. Cyclovoltammetric measurements were performed on a LK98 microcomputer-based electrochemical system (LANLIKE, Tianjin). A three-electrode system was employed, a glass carbon electrode was used as a working electrode and a platinum wire served as the counter electrode and a saturated calomel electrode (SCE) served as the reference electrode. A 0.4 mol L^{-1} NaOAc (pH = 5) buffer was the supporting electrolyte.

2.4. *X-ray structure determination*

Crystallographic data were collected on a Rigaku RAXIS-IV diffractometer with graphite-monochromated Mo-Kα radiation ($\lambda = 0.71073$ Å) at room temperature. The structures were solved by direct methods and refined using full-matrix least squares on F^2. All non-hydrogen atoms were refined anisotropically. All calculations were performed using the SHELXL-97 program [14]. As the quality of these crystals was not good enough for single crystal X-ray analysis to obtain good structural data, the Rint's are comparatively high for both compounds. Crystal and experimental data are listed in table 1, and selected bond distances (Å) of **1** and **2** are given in table 2.

3. Results and discussion

3.1. *Synthesis*

Based on previous work [11, 12], we further explored the synthetic strategy for sandwich-type tungstoantimonates. Compound **1** was synthesized from a cryptate

Table 2. Selected bond lengths (Å) and angles (°) for **1** and **2**.

1		**2**	
Sb1–O36	1.957(12)	Sb1–O33	1.983(15)
Sb1–O35#1	2.009(8)	Sb1–O31	1.998(13)
Sb1–O35	2.009(8)	Sb1–O32	1.999(14)
Sb2–O37#1	1.985(8)	Ni1–O18	2.004(16)
Sb2–O37	1.985(8)	Ni1–O20	2.011(17)
Sb2–O38	1.997(11)	Ni1–O3W	2.039(19)
Cu1–O22	1.930(8)	Ni1–O2W	2.041(16)
Cu1–O22#1	1.930(8)	Ni1–O5#2	2.041(15)
Cu1–O25	1.965(8)	Ni1–O1W	2.07(2)
Cu1–O25#1	1.965(8)	W10–O34	1.76(2)
Cu1–O1w	2.346(12)	W10–O35	1.791(17)
Cu2–O20	1.923(8)	W10–O10#2	1.929(16)
Cu2–O24	1.934(9)	W10–O25	1.949(15)
Cu2–O23	1.942(9)	W10–O28	2.115(15)
Cu2–O21	1.943(8)	W10–O11#2	2.131(16)
Cu2–O2w	2.329(11)		
O22–Cu1–O22#1	90.1(5)	O18–Ni1–O20	82.7(7)
O22–Cu1–O25	90.3(3)	O18–Ni1–O3W	87.5(7)
O25–Cu1–O25#1	88.1(5)	O20–Ni1–O3W	92.4(7)
O22–Cu1–O1W	89.8(4)	O20–Ni1–O2W	92.4(7)
O25–Cu1–O1W	98.3(4)	O3W–Ni1–O2W	90.5(7)
O20–Cu2–O23	91.5(4)	O18–Ni1–O5#2	92.8(6)
O24–Cu2–O23	87.7(4)	O20–Ni1–O5#2	92.2(6)
O20–Cu2–O21	87.0(4)	O2W–Ni1–O5#2	89.6(6)
O24–Cu2–O21	91.9(4)	O18–Ni1–O1W	93.2(7)
O20–Cu2–O2W	93.7(4)	O3W–Ni1–O1W	87.9(8)
O24–Cu2–O2W	98.0(4)	O2W–Ni1–O1W	91.7(7)
O23–Cu2–O2W	97.3(4)	O5#2–Ni1–O1W	87.5(7)
O21–Cu2–O2W	92.4(4)		

Symmetry transformations used to generate equivalent atoms: **(1)** 1: *x*, $-y+1/2$, *z*; #2: $-x+1$, $-y$, $-z+1$. **(2)** #1: $-x-1$, $-y$, $-z$; #2 $-x$, $-y$, $-z$.

$[NaSb_9W_{21}O_{86}]^{18-}$ polyanion avoiding the common *B*-$[SbW_9O_{33}]^{9-}$ precursor. The product contains *B*-$[SbW_9O_{33}]^{9-}$ building blocks, indicating that during the reaction the following transformation must have taken place: $[NaSb_9W_{21}O_{86}]^{18-} \rightarrow$ *B*-α-$[SbW_9O_{33}]^{9-}$. In the synthetic strategy for **2** we did not use any polyoxometalate precursors, but directly employed the raw materials Sb_2O_3, Na_2WO_4 and $NiSO_4$. Under the condition of heating the solution to about 80°C with sodium acetate buffer, the product was obtained with high yield. In the course of the investigation of transition metal substituted sandwich-type tungstoantimonates we discovered that the reaction conditions are more important than the precursor type. Many factors such as the temperature and time of reaction, pH value, ionic strength, concentration of reaction system, influence the type of building blocks and the amount of transition metal incorporated into the core of the sandwich-type compounds. Therefore, further investigation is in progress.

3.2. *Crystal structure*

The crystal structure of **1** shows a sandwich-type polyoxoanion (figure 1 (left)), which consists of two *B*-α-$[SbW_9O_{33}]^{9-}$ subunits linked by three Cu^{2+} ions. Different from

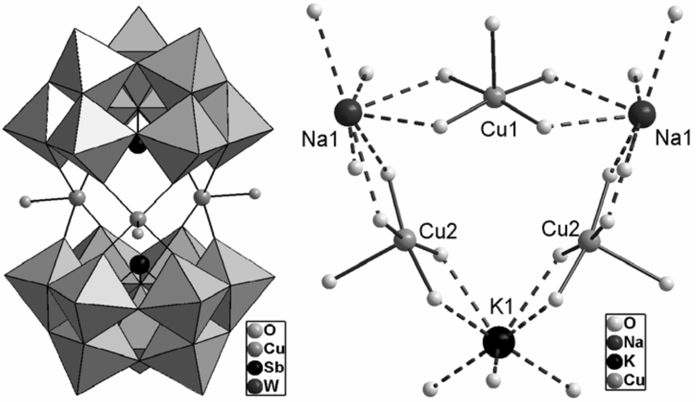

Figure 1. Combined polyhedral/ball-and-stick representation of the polyanion $[\{Cu(H_2O)\}_3(\alpha\text{-}SbW_9O_{33})_2]^{9-}$(left) and ball-and-stick representation of the central belt in **1**(right) . The WO_6 octahedra are shown in dark grey, and hydrogen atoms are omitted for clarity.

previously reported tricopper tungstoantimonates(III) [12], the vacant sites of central belt of the polyoxoanion in **1** are completed by mixed alkali metal cations (two Na^+ and one K^+), which reduces the symmetry of polyoxoanion from C_{3h} to C_{2v}. All copper atoms are square-pyramidally coordinated (Cu–O: 1.923(8)–2.346(12) Å) by four O atoms from two α-$[SbW_9O_{33}]^{9-}$ moieties and one O atom from water. The Sb–O bond lengths are in the narrow range of 1.957(12)–2.009(8) Å. Separation of the two Sb atoms is 4.844 Å due to lone-pair/lone-pair repulsion, in agreement with the previous data ($d_{Sb:Sb} = 4.85$ Å) [12]. However, the distances between the three copper atoms (Cu $\cdots$ Cu, 4.817–4.847 Å) are slightly different, in comparison with the sodium and potassium analogues as a result of the different atomic radius. Furthermore, the two sodium cations in the central belt of **1** are seven-coordinate with six μ_2-oxo atoms and one terminal oxygen from an adjacent polyoxoanion, separating the copper ions (Cu1 and Cu2); the potassium ion (K1) is seven-coordinate by five μ_2-oxo atoms and two waters (see figure 1 (right)). Interestingly, the Na^+ ions bridge two adjacent polyoxoanions forming a 1D chain. Compounds with two different kinds of alkali metal cations incorporated into the central belt of the Hervé-type sandwich-like polyoxoanion framework are rarely reported [15].

The structure of the polyoxoanion $[\{Ni(H_2O)_3\}_2\{W(OH)_2\}_2\{\beta\text{-}SbW_9O_{33}\}_2]^{8-}$ in **2** comprises two *B*-β-$[SbW_9O_{33}]^{9-}$ components joined together via two corner-sharing WO_6 octahedra and two $\{Ni(H_2O)_3\}^{2+}$ units forming a sandwich-like polyoxoanion (figure 2). Compared with three corner-sharing trimetal clusters (W_3O_{13}) fused together in a *B*-α-$[SbW_9O_{33}]^{9-}$ subunit, the *B*-β-$[SbW_9O_{33}]^{9-}$ moiety is formed if one W_3O_{13} triad in *B*-α-$[SbW_9O_{33}]^{9-}$ is rotated by 60°. Each Ni^{2+} ion is bonded to one O atom of one *B*-β-$[SbW_9O_{33}]^{9-}$ moiety and two O atoms of the other, the coordination sphere being completed by three aquo ligands. The Ni–O bond distances range from 2.004(15) to 2.07(2) Å with an average of 2.034 Å, while the O–Ni–O angles vary from 82.7(7)–93.2(7)°. The separation of two Sb atoms (5.646 Å) is longer than in **1** as a result of the half-offset structure. Since the positions of the hydrogen atoms could not be located unambiguously, bond valence sum (BVS) calculations for the relevant O atoms had to be performed [16]. The BVS values of O(34) and O(35) are 1.54 and 1.42, respectively, indicating mono-protonation of these O atoms. This result is different

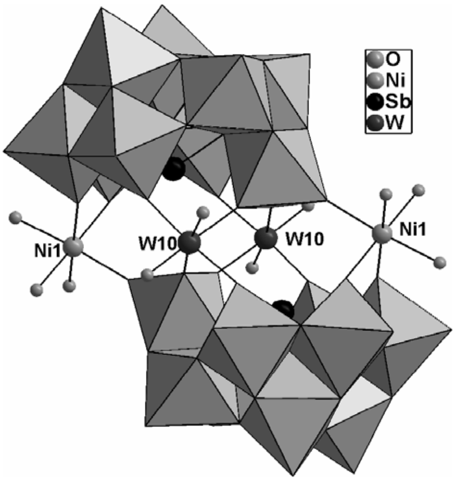

Figure 2. Combined polyhedral/ball-and-stick representation of the polyanion $[\{Ni(H_2O)_3\}_2\{W(OH)_2\}_2\{\beta\text{-}SbW_9O_{33}\}_2]^{8-}$ in **2**. The WO_6 octahedra are shown in dark grey, and hydrogen atoms are omitted for clarity.

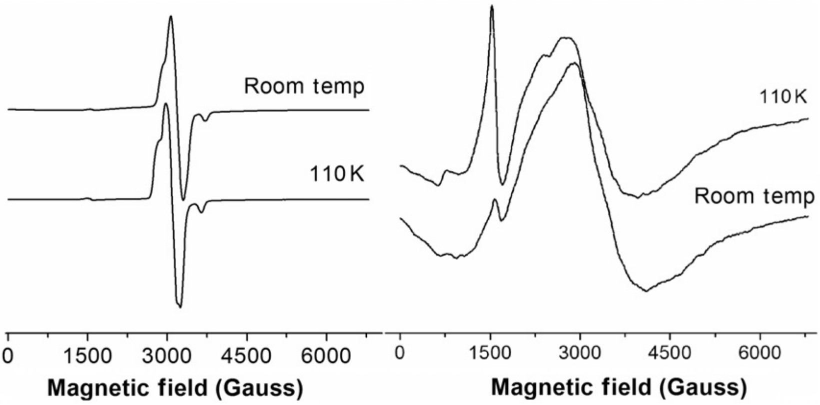

Figure 3. EPR spectra of compounds **1** (left) and **2** (right) at room temperature and at 110 K, respectively.

from data of previously reported antimony analogues [11a]. Moreover, adjacent sandwiched polyoxoanions in **2** are linked by four octahedrally coordinated Na^+ cations forming a chain-like structure.

3.3. *EPR spectra*

Both the room-temperature and the 110 K EPR spectra of **1** as a solid sample shown in figure 3 (left) have a simple isotropic signal at approximately 3100 G. The room-temperature EPR spectrum displays the signal with the effective $g_{iso} = 2.21$, as expected for a distorted square pyramidal geometry around the copper(II) [17]. When the curves are magnified, a very weak signal at about 3600 G, together with a shoulder at 2800 G appears, which is assigned to a very small amount of exchanged (Cu^{2+})

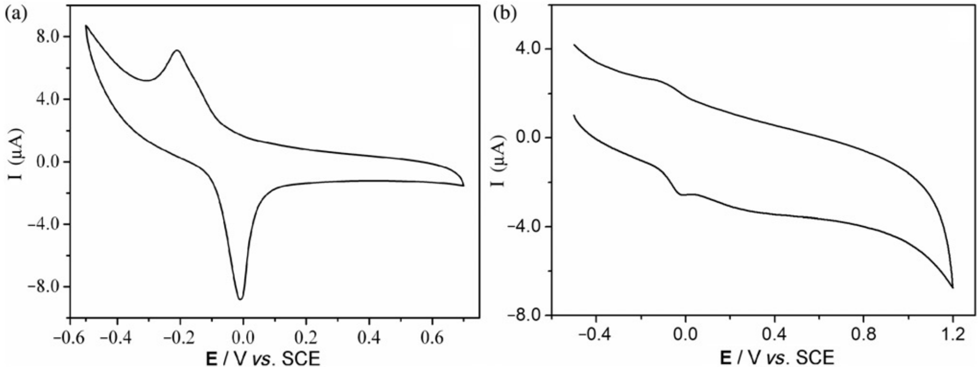

Figure 4. The cyclic voltammogram of $0.1 \times 10^{-3}\,\mathrm{mol\,L^{-1}}$ solutions of compounds **1** (a) and **2** (b) in HOAc-NaOAc buffer (pH = 5); scan rate: $10\,\mathrm{mV\,s^{-1}}$.

species. The values obtained for the principal g tensor are consistent with the structural characteristics of a square-pyramidal environment with the unpaired electron in the $d_{x^2-y^2}$ orbital, typical for the $\{Cu_3\}$-type triangular spin ring [18].

For compound **2** (as shown in figure 3 (right)), the room-temperature EPR spectrum displays an anisotropic broad resonance at approximately 3500 G with an effective $g = 2.01$, and a less intense signal at 1650 G with $g = 4.27$. The extreme signals appearing at $g \approx 4$ and $g \approx 2$ were assigned to a $\Delta M_S = \pm 2$ transition and to a double quantum transition, respectively [19]. The single absorption at very low field of *ca* 870 G is assigned to an axial integer $S = 2$ spin system [20]. The spectra are governed by the usual $S = 1$ spin state and can be interpreted using a rhombic type Hamiltonian $\hat{H} = g\beta HS + D[Sz^2 - S(S+1)/3] + E(Sx^2 - Sy^2)$ [21], where H is the magnetic field vector, g is the spectroscopic splitting factor, β is the Bohr magneton, D is the axial zero field splitting term, E is the rhombic zero field splitting parameter, and S is the electron spin vector. However, when cooling down to 110 K, the resolution is considerably improved, apparently as a result of the signal narrowing induced by the increasing spin-lattice relaxation time and by the existence of strong zero-field splitting (ZFS) within the quartet state.

3.4. *Cyclic voltammetry*

In order to investigate the electrochemical behaviour of compounds **1** and **2**, we carried out cyclovoltammetric (CV) measurements. Figure 4 shows the diagram for $0.1\,\mathrm{mmol\,L^{-1}}$ solutions of **1** and **2** in $0.4\,\mathrm{mol\,L^{-1}}$ NaOAc buffer (pH = 5) as supporting electrolyte. The tungstoantimonate anions exhibit a kinetically stable and reproducible pattern. The CV of **1** shows a pair of well-defined redox waves (reduction potential: −0.213 V and oxidation potential: −0.009 V), which demonstrate that **1** undergoes a one-electron transfer process under this condition with a mid-point peak potential (E_{mid}) of −0.102 V, where $E_{\mathrm{mid}} = (E_{\mathrm{pc}} + E_{\mathrm{pa}})/2$, E_{pc} and E_{pa} are cathodic and anodic peak potentials. The peak potential separation of the redox peaks is 0.201 V, and E_{pc} and E_{pa} values are not dependent on the voltage scan rate, indicating that the one-step reduction process is chemically irreversible. The CV curve of **2** displays a pair of ill-defined redox waves in the same supporting electrolyte solution. Under these conditions, the polyoxoanion of **2** exhibits a nearly reversible one-electron reduction process with a peak-potential separation of approximately 65 mV.

Supplementary data

Further details of the crystal structure investigation may be obtained from Fachinformationszentrum Karlsruhe, 76344 Eggenstein-Leopoldshafen, Germany (Fax: + 49-7247-808-666; Email: crysdata@fiz-karlsruhe.de, http://www.fiz-informationsdienste.de/en/DB/icsd/depot_anforderung.html) on quoting the deposition number CSD-416305 (**1**) and CSD-417379 (**2**).

Acknowledgements

This work was financially supported by the Natural Science Foundation of China, Program for New Century Excellent Talents in University of Henan Province, the Foundation of Education Department of Henan Province, and the Natural Science Foundation of Henan Province.

References

[1] M.T. Pope, A. Müller (Eds), *Polyoxometalate Chemistry: From Topology via Self-Assembly to Applications*, Kluwer, Dordrecht, The Netherlands (2001).

[2] T. Yamase. *Chem. Rev.*, **98**, 307 (1998).

[3] C.L. Hill, C.M. Prosser-McCartha. *Coord. Chem. Rev.*, **143**, 407 (1995).

[4] L.H. Bi, U. Kortz, M.H. Dickman, B. Keita, L. Nadjo. *Inorg. Chem.*, **44**, 7485 (2005).

[5] K. Wassermann, M.H. Dickman, M.T. Pope. *Angew. Chem. Int. Ed.*, **36**, 1445 (1997).

[6] M.T. Pope. *Comput. Coord. Chem. II*, **4**, 635 (2003).

[7] (a) F. Robert, M. Leyrie, G. Hervé. *Acta Crystallogr.*, **B38**, 358 (1982); (b) U. Kortz, S. Nellutla, A.C. Stowe, N.S. Dalal, J. van Tol, B.S. Bassil. *Inorg. Chem.*, **43**, 144 (2004).

[8] (a) T.J.R. Weakley, R.G. Finke. *Inorg. Chem.*, **29**, 1235 (1990); (b) L.H. Bi, E.B. Wang, J. Peng, R.D. Huang, L. Xu, C.W. Hu. *Inorg. Chem.*, **39**, 671 (2000); (c) U. Kortz, S. Nellulta, A.C. Stowe, N.S. Dalal, U. Rauwald, W. Danquah, D. Ravot. *Inorg. Chem.*, **43**, 2308 (2004).

[9] (a) I. Loose, E. Droste, M. Bösing, H. Pohlmann, M.H. Dickman, C. Rosu, M.T. Pope, B. Krebs. *Inorg. Chem.*, **38**, 2688 (1999); (b) U. Kortz, M.G. Savelieff, B.S. Bassil, B. Keita, L. Nadjo. *Inorg. Chem.*, **41**, 783 (2002).

[10] (a) W.H. Knoth, P.J. Domaille, R.D. Farlee. *Organomet.*, **4**, 62 (1985); (b) N. Laronze, J.G. Marrot, G. Hervé. *Inorg. Chem.*, **42**, 5857 (2003).

[11] (a) M. Bösing, I. Loose, H. Pohlmann, B. Krebs. *Chem. Eur. J.*, **3**, 1232 (1997); (b) M. Bösing, A. Nöh, I. Loose, B. Krebs. *J. Am. Chem. Soc.*, **120**, 7257 (1998); (c) F. Hussain, M. Reicke, U. Kortz. *Eur. J. Inorg. Chem.*, 2733 (2004).

[12] (a) P. Mialane, J. Marrot, E. Rivière, J. Nebout, G. Hervé. *Inorg. Chem.*, **40**, 44 (2001); (b) U. Kortz, N.K. Al-Kassem, M.G. Savelieff, N.A. Al-Kadi, M. Sadakane. *Inorg. Chem.*, **40**, 4742 (2001).

[13] G. Hervé, A. Tézé. *Inorg. Synth.*, **27**, 120 (1990).

[14] G.M. Sheldrick. *SHELXL-97, Program for the Refinement*, University of Göttingen, Göttingen, Germany (1997).

[15] L.H. Bi, M. Reicke, U. Kortz, B. Keita, L. Nadjo, R.J. Clark. *Inorg. Chem.*, **43**, 3915 (2004).

[16] I.D. Brown, D. Altermatt. *Acta Crystallogr.*, **B41**, 244 (1985).

[17] D. Li, S. Li, D. Yang, J. Yu, J. Huang, Y. Li, W. Tang. *Inorg. Chem.*, **42**, 6071 (2003).

[18] (a) K.-Y. Choi, Y.H. Matsuda, H. Nojiri. *Phys. Rev. Lett.*, **96**, 107202 (2006); (b) A.C. Stowe, S. Nellutla, N.S. Dalal, U. Kortz. *Eur. J. Inorg. Chem.*, 3792 (2004).

[19] L.A. Pardi, A.K. Hassan, F.B. Hulsbergen, J. Reedijk, A.L. Spek, L.-C. Brunel. *Inorg. Chem.*, **39**, 159 (2000).

[20] S.K. Dey, N. Mondal, M.S. El Fallah, R. Vicente, A. Escuer, X. Solans, M. Font-Bardia, T. Matsushita, V. Gramlich, S. Mitra. *Inorg. Chem.*, **43**, 2427 (2004).

[21] J.J. Girerd, G.C. Papaefthymiou, A.D. Watson, E. Gamp, K.S. Hagen, N. Edelstein, R.B. Frankel, R.H. Holm. *J. Am. Chem. Soc.*, **106**, 5941 (1984).